ChemPubSoc Europe

DOI: 10.1002/ejic.201501355

EurJIC European Journal of Inorganic Chemistry

Full Paper

Redox-Active Ligands

Anthraphen: A Salphen-Like Non-Innocent Tetradentate Anthraquinone Imine Dye – Coordination and Electrochemistry

Christian Prinzisky,[a] Andreas Jacob,[a] Marcus Harrer,[a] Michael Elfferding,[a] and Jörg Sundermeyer*[a]

Abstract: A new, highly redox-active chromophore ligand, H_2(anthraphen) (**1**), containing two *o*-phenylenediamine-linked anthraquinone imine units has been synthesized in a three-step synthesis and fully characterized by X-ray crystallography, UV/Vis spectroscopy, and cyclic voltammetry. The dark-red dye **1** shows molar extinction coefficients of up to 47000 L mol^{-1} cm^{-1} and four reversible reduction processes. This dianionic N_2O_2 ligand, with a significantly extended π system, offers a salphen-like binding cavity for metal coordination, as has been demonstrated by the synthesis of [K_2(anthraphen)] (**2**) and the transition-metal complexes of Ti^{IV} (**3**), V^{IV} (**4**), Fe^{II} (**5**), Fe^{III} (**6**), Co^{II} (**7**), Ni^{II} (**8**), Cu^{II} (**9**), Pd^{II} (**10**), Pt^{II} (**11**), and Zn^{II} (**12**). These metal chromophores have colors ranging from dark-red, violet, green to black. Their optical and electrochemical properties were investigated and compared with those of the diprotic ligand. Coordination led to an increase in the molar extinction coefficients up to 66400 L mol^{-1} cm^{-1} in the case of [V(anthraphen)O] (**4**), broadening of the absorption bands in the visible-light region as well as a redshift of the lowest-energy absorption band. The lowest-energy absorption observed for these complexes to date is for [Ni(anthraphen)] (**8**) at 784 nm. The metal chromophores exhibit up to five fully reversible oxidation and reduction processes.

Introduction

Schiff-base ligands, easily obtained by straightforward condensation reaction of an aldehyde or ketone with a primary amine, have become a basic module of coordination chemistry since their first description by Hugo Schiff in 1864.[1] Metal complexes of these σ-donor and π-acceptor ligands have plenty of applications[2–4] and have been known since the mid-nineteenth century,[5] even before the general preparation of Schiff-base ligands themselves.[1,6]

Probably the most prominent Schiff-base ligand is H_2(salen), obtained by the spontaneous condensation reaction of 2 equivalents of salicylaldehyde with 1 equivalent of ethylenediamine. This tetradentate dianionic ligand was synthesized for the first time by Pfeiffer et al. in 1933.[7] Metal complexes of salen ligands are an important class of compounds and stabilize metals in low as well as higher oxidation states[8–14] due to the π-donor properties of the phenolate and π-acceptor properties of the imine group. Salen complexes have found numerous applications in heterogeneous and homogeneous catalysis, including in the asymmetric epoxidation of olefins by chiral manganese and chromium salen complexes,[9,10] the asymmetric catalysis of epoxide ring-opening reactions,[11,12] and the ring-opening co-polymerization of carbon dioxide and oxiranes to polycarbonates with chromium and cobalt salen complexes.[13,14]

Recently, salen derivatives have attracted great interest because of their redox non-innocent behavior.[15–21] The interplay of redox-active transition-metal ions and pro-radical ligands is an area of considerable research effort because redox processes in some enzymes involve not only metal centers but also coordinated non-innocent ligands[22,23] and also because of their applications in catalysis.[24] Depending on the relative energies of the redox-active orbitals, metal complexes with such non-innocent ligands exist in two limiting descriptions, either as a metal–ligand radical [$M^{n+}(L^{\bullet})$] or as a higher-valent metal–anionic ligand complex [$M^{(n+1)+}(L^{-})$].[19]

Typical examples of non-innocent ligands are *o*-benzohydroquinones (H_2bq),[25–31] which can be oxidized from the doubly deprotonated dianionic catecholate (cat^{2-}) via the radical *o*-benzosemiquinone anion (sbq^{1-}) to the neutral benzoquinone ligand (bq). *o*-Phenylenediamine (H_2pda) and its derivatives are classical examples of non-innocent N-donor ligands.[22,32–34] They can form complexes in the doubly deprotonated dianionic form (pda^{2-}), which in turn can be oxidized to the *o*-benzosemiquinone diiminato radical imino anion ($sbqdi^{1-}$) and to the neutral *o*-benzoquinone diimine ligand (bqdi). Furthermore, *o*-benzoquinone imine (H_2bqi), as a hybrid of *o*-quinone and *o*-phenylenediamine, is an interesting non-innocent ligand[35–37] and has been studied by Pierpont[38] and Wieghardt[39] and their co-workers. Structurally related to *o*-quinones and *o*-quinone imines are *p*-quinones and *p*-quinone imines, respectively (Scheme 1, a).

[a] *Department of Chemistry and Material Sciences Center, Philipps-Universität Marburg, Hans-Meerwein-Straße 4, 35032 Marburg, Germany*
E-mail: jsu@chemie.uni-marburg.de
https://www.uni-marburg.de/fb15/ag-sundermeyer

Supporting information for this article is available on the WWW under http://dx.doi.org/10.1002/ejic.201501355.

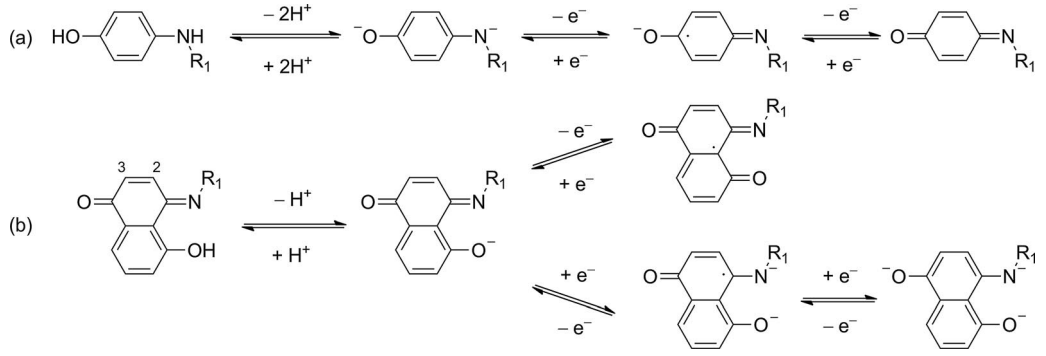

Scheme 1. Different oxidation states of (a) *p*-benzoquinone imine and (b) juglone imine.

Quinone, phenylene diamine, and quinone imine ligands in their ligand-oxidized form are weak σ donors and strong π acceptors. To achieve polydentate *p*-naphthoquinone or *p*-naphthoquinone imine ligands with σ-donor properties like salen derivatives, a hydroxy group has to be introduced into the *peri* position, which leads to juglone and juglone imine derivatives (Scheme 1, b). No transition-metal complexes of juglone imine derivatives have been reported in the literature. For this work we chose the hydroxyanthraquinone motif (Figure 1) to avoid side-reactions at the 2- and 3-positions (Scheme 1, b). Furthermore, anthraquinones are the largest group of naturally occurring quinones. Alizarin, a component of the madder root pigment, has been used as dyestuff since the times of Ancient Egypt and became economically important as the mordant dye Turkey Red in Western Europe in the late medieval centuries. Ancient as well as modern 1-hydroxy-9,10-anthraquinone derivatives are prominent due to their brilliance, color fastness, and photostability as well as for their ability to form, for example, Al and Ca complexes on fibers. This historical background and the fact that no anthraquinone imine complexes have been reported in the literature prompted us to study the condensation reaction of 1-hydroxy-9,10-anthraquinone with phenylene-1,2-diamine, which is by no means a straightforward selective reaction. The targets were non-innocent $[N_2O_2]^{2-}$ hybrid ligands incorporating salphen and anthraquinone building blocks (Figure 1), specifically the tetradentate phenylene-bridged anthraquinone imine *N*,*N*′-bis(1-hydroxy-10-oxo-9-anthryl)-*o*-phenylendiimine, named H_2(anthraphen) (**1**) in the following. Similar to most popular organic chromophore complexes such as metal phthalocyanines or porphyrins, the targeted anthraphen metal dyes may have broad application as redox catalysts, as photophysically active materials in light-driven processes, or as organic semiconductor materials. Here we report the synthesis of the parent ligand **1**, its deprotonation to potassium salt **2**, its coordination chemistry, its structural and chromophore properties, and its electrochemistry within a series of unique transition-metal anthraphen chelate complexes **3**–**12**.

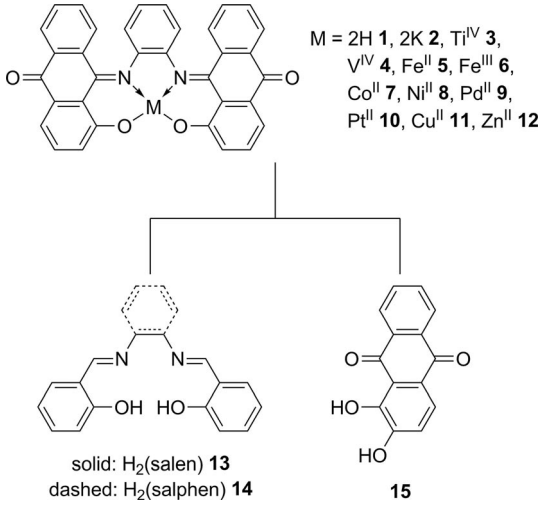

Figure 1. Structural combination of H_2(salphen) (**14**) and alizarin (**15**) to obtain the new tetradentate ligand H_2(anthraphen) (**1**).

Results and Discussion

Synthesis

The direct condensation of 1-hydroxy-9,10-anthraquinone with *o*-phenylenediamine is hampered by the unselective redox reactions of this nucleophile–electrophile pair. The conjugation of the carbonyl groups with the aromatic system and the steric hindrance created by the hydrogen atoms in the *peri* positions causes ordinary 9,10-anthraquinones to react only with strong and hard nucleophiles under harsh conditions.[40] Our synthesis of the tetradentate H_2(anthraphen) (**1**) follows a three-step procedure (Scheme 2) involving the literature-known regioselective activation of the keto function in the *peri* position by the mediating hydroxy group.[41,42] 1-Hydroxyanthraquinone (**16**) was treated with acetic anhydride to form 1-acetoxy-9,10-anthraquinone (**17**), thereby introducing an acetoxy group as auxiliary (Y_p = 98 %) that facilitates and controls the selective nucleophilic substitution at the 9-position (for numbering see Figure 2). The second step leads, by migration of the acetoxy group in alkaline media using sodium methoxide in tetrahydrofuran/methanol, to the dimethoxy acetal **18**.[40,43,44] After work-

up with acetic acid, the pure 1-hydroxy-9,9-dimethoxy-10-anthrone (**18**) can be isolated by column chromatography on deactivated silica gel (Y_p = 69 %). These two steps are necessary to activate the system for the subsequent condensation reaction. Furthermore, these two steps are essential to selectively substitute the 9-carbonyl. An alternative route[45] using phosphorus pentachloride was also tested but led to lower yields. H_2(anthraphen) (**1**) was obtained by the reaction of 1-hydroxy-9,9-dimethoxy-10-anthrone (**18**) with 0.5 equivalents of *o*-phenylenediamine (**19**) in toluene at reflux and was purified by column chromatography (Y_p = 72 %).

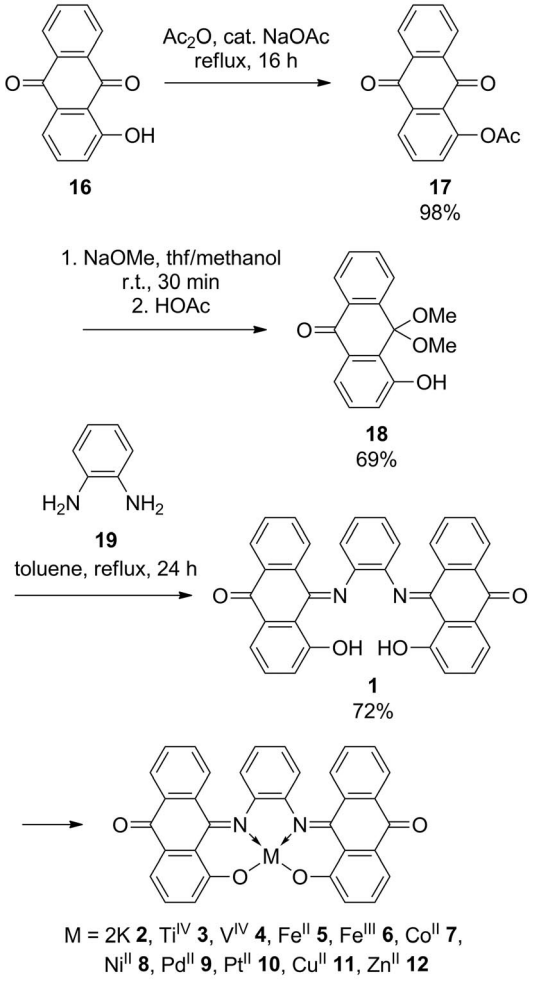

Scheme 2. Synthesis of H_2(anthraphen) (**1**) and its complexes **2**–**12**.

Subsequently, H_2(anthraphen) (**1**) was treated with a series of metal cations. Depending on the cation, the corresponding acetates, acetylacetonates, or amides were used for the metalation processes (Table 1). In the case of iron(III), the corresponding metal halide was used, which reacted with the ligand after its deprotonation with potassium bis(trimethylsilyl)amide.

For most substances, single crystals suitable for XRD were obtained. Unless stated otherwise, all compounds were analyzed by NMR, IR, and UV/Vis spectroscopy, mass spectrometry, cyclic voltammetry, and elemental analysis.

Table 1. Synthesized metal complexes, reagents used, reaction conditions, and product yields for **2**–**12**.

Compound[a]	Reagents	Solvents and conditions	Y_p [%]
[K_2(ap)] (**2**)	KH	thf, r.t., 1 h	58
[Ti(ap)(NMe_2)$_2$] (**3**)	Ti(NMe_2)$_2$	toluene, reflux, 0.5 h	86
[V(ap)O] (**4**)	[VO(acac)$_2$]	toluene, reflux, 18 h	86
[Fe(ap)] (**5**)	[Fe(hmds)$_2$(thf)]	thf, reflux, 0.5 h	93
[Fe(ap)Cl] (**6**)	1. [K(hmds)]	toluene, reflux, 0.5 h	72
	2. $FeCl_3$	thf, reflux, 1 h	
[Co(ap)] (**7**)	[Co(hmds)$_2$(thf)]	toluene, reflux, 2.5 h	91
[Ni(ap)] (**8**)	Ni(OAc)$_2$·4H_2O	methanol, reflux, 3.5 h	88
[Pd(ap)] (**9**)	Pd(OAc)$_2$	methanol, reflux, 3 h	93
[Pt(ap)] (**10**)	1. NaOAc	dmf, r.t., 15 min	20
	2. Zeise's dimer[b]	110 °C, 4 d	
[Cu(ap)] (**11**)	Cu(OAc)$_2$·H_2O	methanol, reflux, 3.5 h	85
[Zn(ap)] (**12**)	[Zn(hmds)$_2$]	toluene, reflux, 1.5 h	62

[a] ap: anthraphen. [b] Zeise's dimer: [{PtCl(C_2H_4)}(μ-Cl)]$_2$.

NMR Spectroscopy

The diamagnetic compounds 1-acetoxy-9,10-anthraquinone (**17**), 1-hydroxy-9,9-dimethoxy-10-anthrone (**18**), H_2(anthraphen) (**1**), [Ti(anthraphen)(NMe_2)$_2$] (**3**), [Ni(anthraphen)] (**8**), [Pd(anthraphen)] (**9**), [Pt(anthraphen)] (**10**), and [Zn(anthraphen)] (**12**) were analyzed by NMR spectroscopy (but not [K_2(anthraphen)] (**2**) due to its poor solubility in common solvents). These compounds were fully characterized by ^{1}H and ^{13}C NMR spectroscopy, and all signals were chemically unequal and so a full assignment was carried out by means of 2D COSY, HMQC, and HMBC experiments, except for [Ti(anthraphen)(NMe_2)$_2$] (**3**) and [Pt(anthraphen)] (**10**), for which no reasonable data were obtained due to their low solubility. All ^{1}H, ^{13}C, and 2D NMR spectra are presented in the Supporting Information.

Mass Spectrometry

The precursors **17** and **18**, the ligand **1**, and the metal complexes **3**–**12**, but not the potassium salt **2**, were analyzed by mass spectrometry. Compounds **17** and **18** were ionized by electrospray ionization, whereas ligand **1** and the complexes **3**–**12** were ionized by atmospheric-pressure chemical ionization (APCI). All the data and high-resolution mass spectra can be found in the Supporting Information.

Single-Crystal XRD Structures

Single crystals of H_2(anthraphen) (**1**), [V(anthraphen)O] (**4**), [Fe(anthraphen)Cl] (**6**), [Co(anthraphen)] (**7**), [Ni(anthraphen)] (**8**), [Pd(anthraphen)] (**9**), [Pt(anthraphen)] (**10**), [Cu(anthraphen)py] (**11**), and [Zn(anthraphen)] (**12**) were obtained and analyzed by XRD. Single crystals of **1** were grown by slow evaporation from a saturated toluene solution, **4** and **7** by diffusion of pentane into a saturated dichloromethane solution, **6** by cooling a saturated tetrahydrofuran solution from room temperature to –20 °C, **8**, **10**, and **12** by slow evaporation from saturated tetrahydrofuran solutions, **9** by the diffusion of pentane into a saturated tetrahydrofuran solution, and **11** by slow evaporation from a saturated pyridine solution.

The numbering of the anthraquinone imine structure is in accord with IUPAC, and is shown in Figure 2. Additional crystallographic data and experimental parameters are listed in the Supporting Information.

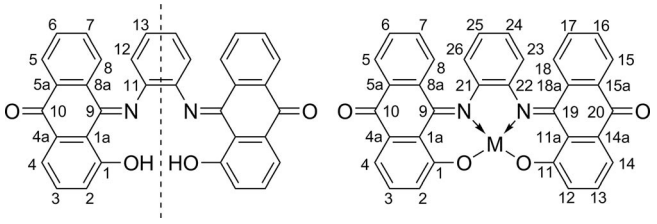

Figure 2. Numbering of the H_2(anthraphen) ligand **1** (left) and the metal–anthraphen complexes **2**–**12** (right).

The tetradentate H_2(anthraphen) ligand (**1**) crystallizes in the monoclinic space group *C*2/*c* and the asymmetric unit consists of half a molecule with crystallographically induced mirror symmetry. The parameters of the intramolecular hydrogen bond between O–H as donor and N as acceptor [*d*(O1···N1) = 2.537(3) Å; <(O1H1N1) = 156(3)°; Figure 3a] are in the same range as those of H_2(salen) [*d*(O1···N1) = 2.596(2) Å; <(O1H1N1) = 146.0°][46] and H_2(salphen) [*d*(O1···N1) = 2.564 Å; <(O1H1N1) = 150.0°].[47]

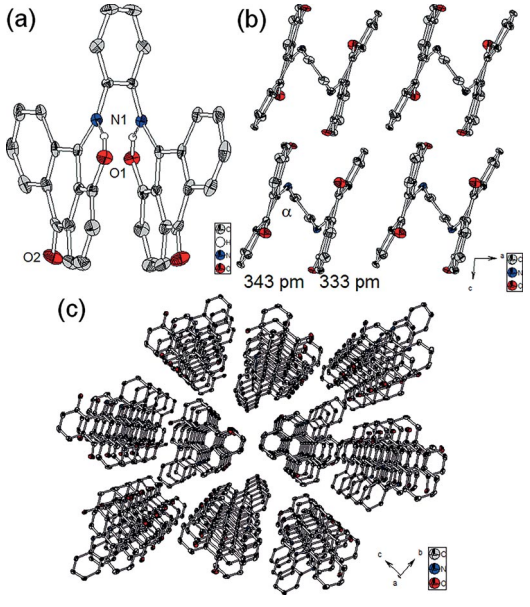

Figure 3. (a) Molecular structure, (b) illustration of intra- and intermolecular π stacking, and (c) column-like structure of H_2(anthraphen) (**1**).

Furthermore, it is notable that the two anthraquinone imine moieties show intermolecular (shortest distance found: 3.33 Å) as well as intramolecular (shortest distance found: 3.43 Å) π stacking (Figure 3, b). As a result of the π stacking, H_2(anthraphen) (**1**) forms a column-like structure (Figure 3, c). The angle *α* of 56.1° between the phenylene bridge and the carbon atoms of the quinone imine moieties (Figure 3, b) indicates weak π conjugation in the aromatic systems.

[V(anthraphen)O] (**4**) crystallizes in the monoclinic space group $P2_1/c$, with two complex molecules and several disordered dichloromethane molecules in the asymmetric unit, [Fe(anthraphen)Cl] (**6**, $P2_1/n$) crystallizes with one complex molecule in the asymmetric unit, [Co(anthraphen)] (**7**, $P2_1/c$) crystallizes with one complex and one dichloromethane molecule in the asymmetric unit, and [Ni(anthraphen)] (**8**, $P2_1/c$) crystallizes with one complex and one tetrahydrofuran molecule in the asymmetric unit. [Pd(anthraphen)] (**9**, $P2_1/n$) crystallizes with one complex and half a tetrahydrofuran molecule in the asymmetric unit. The half tetrahydrofuran molecule is disordered through an inversion center. It should be noted that the reflection data show a low ratio of observed/unique reflections of 46 %. [Pt(anthraphen)] (**10**, $P2_1/c$) crystallizes isostructurally to [Co(anthraphen)] (**7**), with one complex and one dichloromethane molecule in the asymmetric unit, [Cu(anthraphen)py] (**11**, $P2_1/c$) crystallizes with one complex pyridine adduct, one water, and one disordered pyridine molecule in the asymmetric unit, and [Zn(anthraphen)] (**12**) crystallizes in the triclinic space group $P\bar{1}$. The molecular structures of **4** and **6**–**12** are shown in Figure 4.

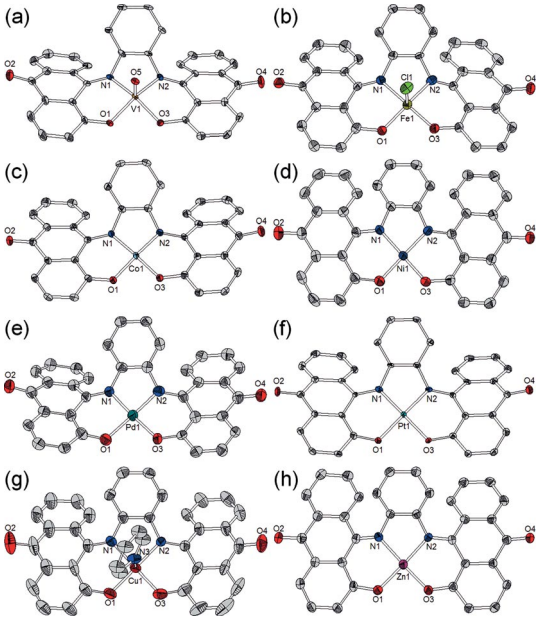

Figure 4. Molecular structures of (a) [V(anthraphen)O] (**4**), (b) [Fe(anthraphen)Cl] (**6**), (c) [Co(anthraphen)] (**7**), (d) [Ni(anthraphen)] (**8**), (e) [Pd(anthraphen)] (**9**), (f) [Pt(anthraphen)] (**10**), (g) [Cu(anthraphen)py] (**11**), and (h) [Zn(anthraphen)] (**12**). For clarity, solvent molecules and hydrogen atoms are not shown. Note that the pyridine molecule of [Cu(anthraphen)py] (**11**) had to be constrained and restrained with the commands EADP and ISOR.

The complexes show weak intermolecular hydrogen bonds between C–H as donor and O as acceptor (see the Supporting Information). Furthermore, intermolecular π stacking can be observed for [Co(anthraphen)] (**7**), [Ni(anthraphen)] (**8**), and [Pt(anthraphen)] (**10**; Figure 5, a–c). [Co(anthraphen)] (**7**) and [Pt(anthraphen)] (**10**) also show column-like structures with alternating Co–Co distances of 6.8754 and 3.3612 Å and Pt–Pt distances of 6.7429 and 3.3076 Å, respectively (Figure 5, a,b). The shorter Co–Co and Pt–Pt distances indicate intermolecular π stacking between the quinone imine moieties (Figure 5, b). [V(anthraphen)O] (**4**), [Fe(anthraphen)Cl] (**6**), [Cu(anthraphen)py] (**11**), and [Zn(anthraphen)] (**12**) show column-like structures (Figure 5, d–g), but with no clearly identifiable π

stacking due to the strong bending of the anthraquinone imine structure and in the case of [V(anthraphen)O] (**4**) due to interactions with numerous solvent molecules. For [Pd(anthraphen)] (**9**), neither π stacking nor a column-like structure was observed.

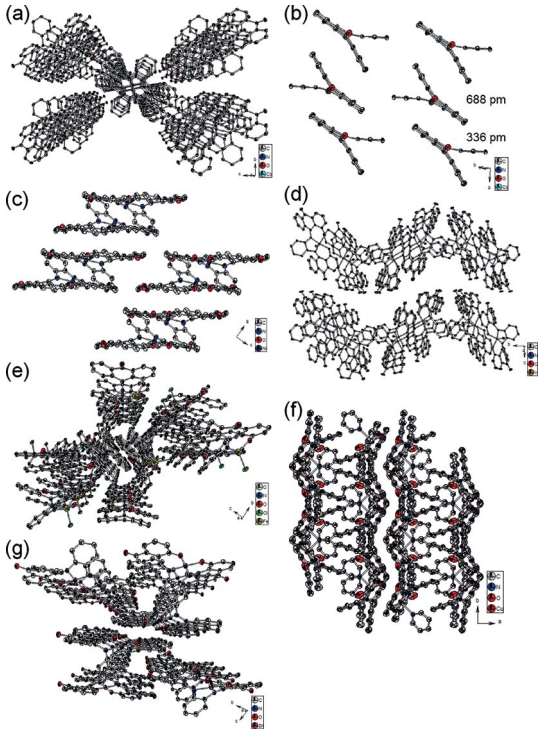

Figure 5. (a) Column-like structure and (b) π stacking of [Co(anthraphen)] (**7**) {isostructural with [Pt(anthraphen)] (**10**)}, (c) π stacking of [Ni(anthraphen)] (**8**) and column-like structures of (d) [V(anthraphen)O] (**4**), (e) [Fe(anthraphen)Cl] (**6**), (f) [Cu(anthraphen)py] (**11**), and (g) [Zn(anthraphen)] (**12**). For clarity, hydrogen atoms and solvent molecules are not shown.

The N–M and O–M bond lengths of the metal complexes and those of comparable literature-known salen complexes are listed in Table 2. Comparison shows that the bond lengths are nearly identical. Larger differences are observed for the zinc complexes due to strong intermolecular interactions of the solvent-free salen complex, which result in a binuclear complex. Short contacts are formed between O1 and the metal center of a second complex molecule, which result in longer O–M and N–M bonds. Furthermore, the copper–anthraphen complex shows shorter N–M but longer O–M distances, which can be explained by the influence of the axial pyridine ligand and enhanced coordination number.

The coordination geometries of the metal atoms can be determined by comparison of the torsion angles of the donor atoms O1–N1–N2–O3 {also O6–N3–N4–O8 for [V(anthraphen)O] (**4**)}, the positions of the metal atom relative to the plane formed by them, and the M–L_{axial} bond lengths in the case of [V(anthraphen)O] (**4**), [Fe(anthraphen)Cl] (**6**), and [Cu(anthraphen)py] (**11**). The relevant values are listed in Table 3. Also listed are comparable M–L_{axial} bond lengths of literature-known salen complexes. It is incidental that four different coordination geometries are obtained. The nickel, palladium, and platinum atoms have a square-planar configuration typical of low-spin d^8 metal complexes, the cobalt and zinc atoms have a distorted square-planar configuration, the vanadium atom has a square-pyramidal configuration, and the iron and copper atoms have a distorted square-pyramidal configuration.

Table 2. Bond lengths of the anthraphen and literature-known salen complexes.

Compound[a]	*d*(N1–M) [Å]	*d*(N2–M) [Å]	*d*(O1–M) [Å]	*d*(O3–M) [Å]
[V(ap)O] (**4**)	2.080(4)	2.081(4)	1.921(3)	1.902(3)
	2.083(4)	2.081(4)	1.897(4)	1.918(3)
[V(salen)O][48]	2.046(1)	2.054(1)	1.921(1)	1.922(1)
	2.055(1)	2.057(1)	1.924(1)	1.925(1)
[Fe(ap)Cl] (**6**)	2.131(4)	2.131(5)	1.882(4)	1.869(4)
[Fe(salen)Cl][49]	2.098(9)	2.091(10)	1.898(7)	1.978(7)
[Co(ap)] (**7**)	1.874(2)	1.8806(19)	1.8303(16)	1.8282(17)
[Co(salen)][50]	1.88(1)	1.88(1)	1.88(1)	1.95(1)
[Ni(ap)] (**8**)	1.864(3)	1.873(3)	1.832(2)	1.817(2)
[Ni(salen)][51]	1.8519(10)	1.8494(10)	1.8494(10)	1.8540(8)
[Pd(ap)] (**9**)	1.974(5)	1.962(5)	1.976(4)	1.970(4)
[Pd(salen)][52]	1.952(2)	1.957(2)	1.9981(16)	2.0087(16)
[Pt(ap)] (**10**)	1.967(4)	1.972(3)	1.982(3)	1.973(3)
[Pt(salen)][53]	1.938(5)	1.950(5)	2.006(4)	2.002(4)
[Cu(ap)py] (**11**)	1.898(5)	1.900(5)	1.980(5)	1.983(5)
[Cu(salen)][54][b]	1.958(2)	1.959(2)	1.945(2)	1.911(2)
[Zn(ap)] (**12**)	1.952(3)	1.947(3)	1.885(3)	1.884(2)
$[Zn(salen)]_2$[55]	2.072(5)	2.078(6)	2.053(5)	2.053(5)

[a] ap: anthraphen. [b] In the case of the copper–salen complex, no pyridine adduct has been found in the literature and so solvent-free [Co(salen)] has been used for comparison.

Table 3. Torsion angles (γ) of the donor atoms O1–N1–N2–O3, positions of the metal atom relative to the plane (Pl) formed by them, M–L_{axial} bond lengths, angles α between the planes formed by C21–C26 and C1a–C4a–C10–C5a–C8a–C9, angles β formed by C21–C26 and C11a–C14a–C20–C15a–C18a–C19, and ionic radius of the metal cation.

Compound[a]	γ [°]	*d*(M···Pl) [Å]	*d*(M–L) [Å]	α [°], β [°]	*αβ* [°]
H_2(ap) (**1**)				56.1	56.1
[V(ap)O] (**4**)	0.12	0.58	1.601(3)	45.9	46.1
	0.10	0.58	1.606(3)	45.6	
				47.2	
				45.8	
[V(salen)O][48]			1.590		
[Fe(ap)Cl] (**6**)	3.40	0.56	2.2125(16)	47.5	48.5
				49.5	
[Fe(salen)Cl][49]			2.295		
[Co(ap)] (**7**)	2.24	0.06		44.1	44.8
				45.4	
[Ni(ap)] (**8**)	0.00	0.03		45.4	44.9
				44.3	
[Pd(ap)] (**9**)	0.26	0.03		54.6	50.8
				47.1	
[Pt(ap)] (**10**)	0.53	0.06		43.8	44.3
				44.8	
[Cu(ap)py] (**11**)	1.02	0.16	2.335(6)	50.0	49.5
				49.0	
[Zn(ap)] (**12**)	2.94	0.01		46.3	44.4
				42.4	

[a] ap: anthraphen.

The interplanar angle *α* between the phenylenediamine bridge and the carbon atoms of the quinone imine system has already been discussed above for H_2(anthraphen) (**1**; Figure 3, b). The corresponding angles *α* and *β* for the metal complexes **4**,**6**–**12** are listed in Table 3. No distinctive trend can be identified between the metal complexes. On the one hand, Cu^{2+} and

Pd^{2+} have the largest ionic radii and their complexes show the largest average angles. On the other hand, nickel and vanadium have the smallest ionic radii and their complexes show medium-to-high average angles. Zinc, platinum, and cobalt have medium ionic radii and their complexes also show medium average angles.[56] All in all, the interplanar angles within these chelate complexes are significantly smaller than that of the protonated ligand. In contrast to phthalocyanine [PcM] complexes, the title compounds [M(ap)] cannot be perfectly planar as the aromatic hydrogen atoms C8–H and C26–H as well as C18–H and C23–H avoid facing each other.

UV/Vis Spectroscopy

The absorption spectra of H_2(anthraphen) (**1**), [Ti(anthraphen)$(NMe_2)_2$] (**3**), [V(anthraphen)O] (**4**), [Fe(anthraphen)] (**5**), [Fe(anthraphen)Cl] (**6**), [Co(anthraphen)] (**7**), [Ni(anthraphen)] (**8**), [Pd(anthraphen)] (**9**), [Cu(anthraphen)] (**11**), and [Zn(anthraphen)] (**12**) in dichloromethane are shown in Figure 6 and their corresponding absorption maxima and molar extinction coefficients are presented in Table 4. For the platinum (**10**) and potassium (**2**) complexes no meaningful spectra could be obtained due to their very low solubility in dichloromethane and other common solvents.

All the compounds show their strongest absorption bands in the short-wavelength region at 250 ± 5 nm, which is believed to be due to a π→π* transition of the benzenoid system based on comparison with the data of anthraquinone derivatives.[57] A second weak absorption at 322 ± 12 nm can be found as a shoulder for H_2(anthraphen) (**1**), [Co(anthraphen)] (**7**), and [Ni(anthraphen)] (**8**), or as an isolated peak for [Fe(anthraphen)] (**5**), [Pd(anthraphen)] (**9**), and [Cu(anthraphen)] (**11**), which can also be correlated to a benzenoid absorption.[57] Furthermore, most of the compounds show a medium-intense absorption band at 291 ± 9 nm, which is believed to originate from quinone iminoid electron transfer.[57] Weak quinonoid absorption is also mentioned in the literature at 405 nm, which can be correlated to the absorption at 435 ± 1 nm for the quinone iminoid system. It is also known for salen derivatives that the free ligand shows an n→π* transition in the region of 400–440 nm that involves the promotion of a free lone-pair electron on the nitrogen atom to an antibonding π* orbital of the imine group.[58,59] The absorption of [Ti(anthraphen)$(NMe_2)_2$] (**3**), [Ni(anthraphen)] (**8**), and [Zn(anthraphen)] (**12**) in that wavelength range could be due to a d→π* transition.[60] The absorption bands between 461 and 748 nm, depending on the central metal atom, can be explained qualitatively by d→d transitions. The electronic spectrum of [Co(anthraphen)] (**7**), for example, is typical of a Co^{II} d^7 complex with d→d transitions at 410–490 nm and higher wavelengths.[60] The UV/Vis spectrum of [Ni(anthraphen)] (**8**) is typical of a low-spin d^8 square-planar group 10 complex with d→d transitions at 500 nm and a higher wavelength.[61] The electronic spectrum of [Cu(anthraphen)] (**11**) is typical of a Cu^{II} d^9 complex with a d→d transition at around 580 nm,[18] which fits with the broad absorption between 500–600 nm. The complete assignment is hindered because of overlapping π→π* and d→π* or d→d transitions in this versatile system. It is notable that all the complexes show higher molar extinction coefficients than the free ligand.

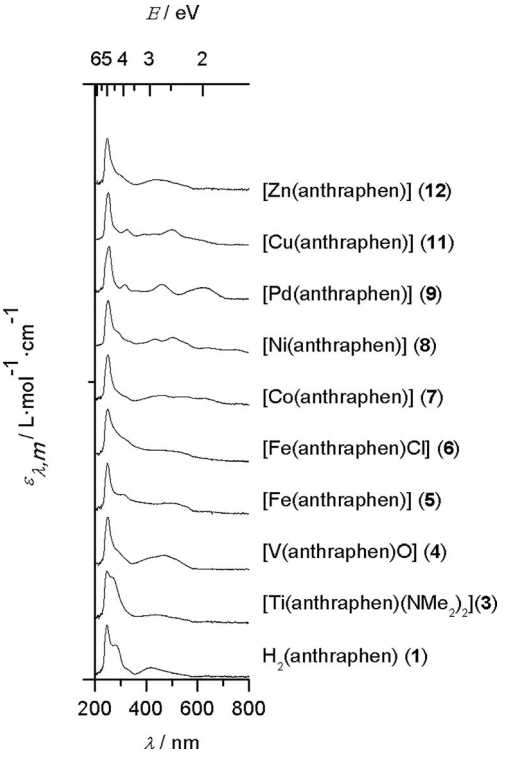

Figure 6. UV/Vis spectra of H_2(anthraphen) (**1**), [Ti(anthraphen)$(NMe_2)_2$] (**3**), [V(anthraphen)O] (**4**), [Fe(anthraphen)] (**5**), [Fe(anthraphen)Cl] (**6**), [Co(anthraphen)] (**7**), [Ni(anthraphen)] (**8**), [Pd(anthraphen)] (**9**), [Cu(anthraphen)] (**11**), and [Zn(anthraphen)] (**12**) in dichloromethane.

Table 4. Absorption data for H_2(anthraphen) (**1**) and its complexes **3**–**9**, **11**, and **12**.

Compound[a]	λ [nm] (ε [L mol^{-1} cm^{-1}])[b]							
	1	2	3	4	5	6	7	8
H_2(ap) (**1**)	252 (47000)	282 (31100)	325	435 (11400)				
[Ti(ap)$(NMe_2)_2$] (**3**)	246 (49800)	265 (45900)		434 (11100)				
[V(ap)O] (**4**)	250 (66400)	288			470 (19300)			
[Fe(ap)] (**5**)	249 (57500)		310 (26700)	386	470 (16000)			
[Fe(ap)Cl] (**6**)	250 (38900)	300			473			
[Co(ap)] (**7**)	251 (61100)		317		461 (15600)	558 (13500)	612 (11500)	
[Ni(ap)] (**8**)	252 (61700)	282	334	435 (20200)	504 (22200)	553	640	748
[Pd(ap)] (**9**)	255 (55700)		316 (17500)		463 (17100)		619 (13400)	
[Cu(ap)] (**11**)	253 (65100)	284	326 (22700)	394	501 (22300)		592	
[Zn(ap)] (**12**)	248 (63900)	299		434 (18.900)				

[a] ap: anthraphen. [b] In the case of shoulders, the approximate wavelengths of the theoretical maxima are given without molar extinction coefficients.

Figure 7 shows the UV/Vis spectra of H_2(anthraphen) (**1**), as the free ligand, [Ni(anthraphen)] (**8**), as the complex showing the highest molar extinction coefficients, and [Pd(anthraphen)] (**9**), as the complex with an absorption in the longest wavelength region for comparison. [Ni(anthraphen)] (**8**) shows at 252 nm with ε = 61700 L mol^{-1} cm^{-1} an extinction coefficient nearly twice as high as that of the free ligand **1**. Furthermore, all extinction coefficients are increased, and another absorption maximum is evident at 504 nm with a shoulder at 553 nm along with weak absorptions at 640 and 748 nm. The palladium complex **9** shows less of an increase in absorbance, but therefore a broader absorption between 463 and 619 nm. The latter could be caused by d→d transitions.

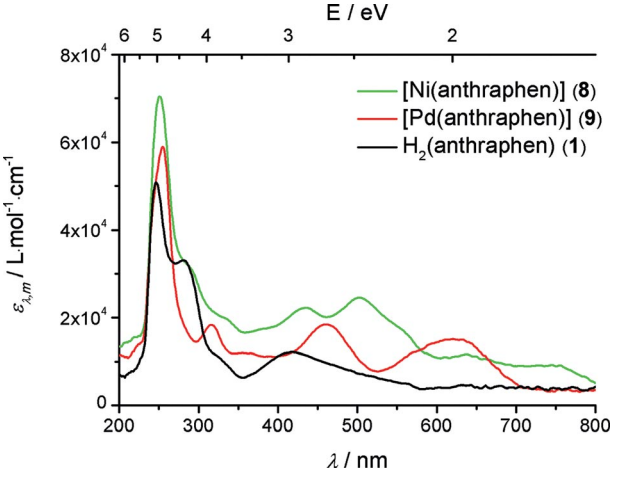

Figure 7. UV/Vis spectra of H_2(anthraphen) (**1**), as free ligand, [Ni(anthraphen)] (**8**), as the complex showing the highest molar extinction coefficients, and [Pd(anthraphen)] (**9**), as the complex with an absorption in the longest wavelength region.

Complexes of salen derivatives have molar extinction coefficients of approximately 10000 L mol^{-1} cm^{-1},[62] whereas the H_2(anthraphen) complexes **2**–**12** show molar extinction coefficients of up to 66400 L mol^{-1} cm^{-1}.

Cyclic Voltammetry

The redox behavior of H_2(anthraphen) (**1**), [V(anthraphen)O] (**4**), [Fe(anthraphen)Cl] (**6**), [Co(anthraphen)] (**7**), [Ni(anthraphen)] (**8**), [Pd(anthraphen)] (**9**), [Cu(anthraphen)] (**11**), and [Zn(anthraphen)] (**12**) was investigated by cyclic voltammetry. [K_2(anthraphen)] (**2**), [Ti(anthraphen)(NMe_2)$_2$] (**3**), [Fe(anthraphen)] (**5**), and [Pt(anthraphen)] (**10**) could not be investigated because of their low solubility. Figure 8 shows exemplarily the cyclic voltammogram of H_2(anthraphen) (**1**). The redox potentials Φ^1_{rev} and peak separation values $\Delta\Phi(j_p^a–j_p^k)$ determined from all the cyclic voltammetry experiments are summarized in Table 5; high-resolution graphics can be found in the Supporting Information. From the peak separation values and the cathodic-to-anodic or anodic-to-cathodic peak current ratios, the electron-transfer mechanisms were estimated to be reversible, quasi-reversible, or irreversible, and consist of one or multiple electron transfers. All the compounds were investigated at different scan rates to determine the dependencies of the peak current, which gives information about the kinetics of the processes. Thereby a diffusion-controlled electron-transfer process can be confirmed (Figure 9).

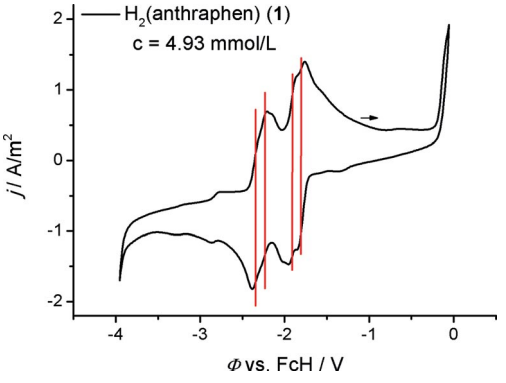

Figure 8. Cyclic voltammogram of [H_2(anthraphen)] (**1**) in DMSO (ca. 5 mmol L^{-1}) with $TBAPF_6$ (50 mmol L^{-1}) as electrolyte at a scan rate of 50 mV s^{-1}. Potentials are plotted against the ferrocene/ferrocenium redox couple. The arrow indicates the starting point and scan direction.

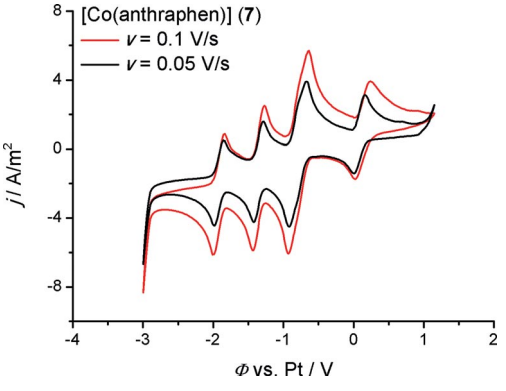

Figure 9. Cyclic voltammograms of [Co(anthraphen)] (**7**) recorded at different scan rates.

Table 5. Redox potentials Φ^1_{rev} vs. FcH and peak separation values $\Delta\Phi(j_p^a–j_p^k)$ in DMSO with $TBAPF_6$ as electrolyte.[a]

Compound[b]	Φ_{rev} [V] {$\Delta\Phi(j_p^a–j_p^k)$ [mV]}				
	1	2	3	4	5
H_2(ap) (**1**)	–1.81 {91}	–1.91 {89}	–2.24 {60}	–2.36 {60}	
[V(ap)O] (**4**)	0.24 {88}	–0.78	–0.97 {110}	–1.30 {72}	–1.97 {73}
[Fe(ap)Cl] (**6**)	–0.58 {111}	–1.18 {140}			
[Co(ap)] (**7**)	–0.28 {160}	–1.09 {131}	–1.22 {119}	–1.71 {130}	–2.28 {130}
[Ni(ap)] (**8**)	–1.95 {130}	–2.53 {150}	–2.91 {140}		
[Pd(ap)] (**9**)	–0.95 {109}	–1.19 {119}	–1.75 {109}	–2.08 {111}	
[Cu(ap)] (**11**)	–0.88 {90}	–1.39 {70}	–1.68 {69}	–2.13 {80}	
[Zn(ap)] (**12**)	–1.38 {111}	–1.63 {111}	–1.88 {110}	–2.08 {140}	

[a] All potentials represent a one-electron redox event. [b] ap: anthraphen.

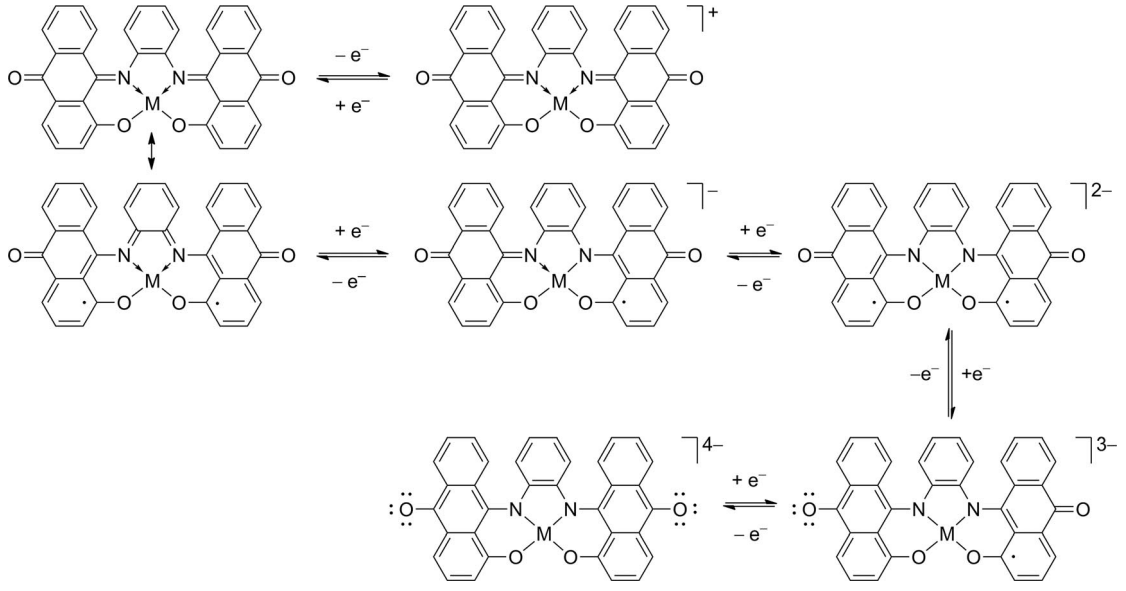

Scheme 3. Schematic illustration of four ligand-centered reduction and one metal-centered oxidation processes.

The ligand, H_2(anthraphen) (**1**), shows two times, two superimposed reversible charge transfers (–1.81, –1.91, –2.24, –2.36 V). It is notable that the ligand is able to take up reversibly four electrons without decomposition. The overlapping redox processes can be explained by the structure of the ligand. As proven by the crystal structure, the two anthraquinone imine units are not perfectly conjugated through the phenylenediamine bridge. As a consequence, electronically, two relatively independent and equal π-conjugated systems exist. The system will change its conformation on taking up one electron and so a small shift is observed for the take-up of the second electron (Figure 8). The cyclic voltammogram of [V(anthraphen)O] (**4**) shows four reversible redox processes (0.24, –0.97, –1.30, –1.97 V) and one quasi-reversible charge transfer (–0.78 V). It can be assumed that the missing reduction process of the quasi-reversible charge transfer is overlapped by the redox process at –0.97 V, which could explain the high peak separation of 110 mV compared with the other four processes (80 ± 8 mV). [Fe(anthraphen)Cl] (**6**) shows two reversible processes (–0.58, –1.18 V) and two broad peaks. This observation can be explained by the poor solubility of **6**, which resulted in residual solid in the sample. All further samples were filtered through a 0.45 μm Teflon syringe filter before measurement. [Co(anthraphen)] (**7**) shows two reversible (–1.71, –2.28 V), two overlapped reversible (–1.09, –1.22 V), and one quasi-reversible redox process (–0.28 V). A clear localization of the redox events within the structure could not be achieved. The supposed structures of four ligand-centered reduction and one metal-centered oxidation processes are illustrated in Scheme 3. In the case of the cobalt complex **7**, a nonligand-centered Co^{II} to Co^{III} oxidation at –0.28 V was estimated based on a comparison with Co(salen) complexes.[63,64] The comparisons also indicate that the metal complexes **4**, **6**–**9**, **11**, and **12** of H_2(anthraphen) (**1**) show high stability against reduction and oxidation. Up to four electrons can be taken up and released reversibly.

[Ni(anthraphen)] (**8**) shows two reversible redox processes (–2.53, –2.91 V) and one quasi-reversible process (–1.95 V). Weak processes also occur at voltages in the range –0.5 to –1.5 V (vs. FcH) that cannot be explained. However, after a few cycles, the cyclic voltammogram seems to be identical to the first cycle. [Pd(anthraphen)] (**9**) and [Cu(anthraphen)] (**11**) show four reversible reduction processes (Pd: –0.95, –1.19, –1.75, –2.08 V; Cu: –0.88, –1.39, –1.68, –2.13 V) whereas [Zn(anthraphen)] (**12**) shows three reversible and one quasi-reversible reduction processes (–1.38, –1.63, –1.88, –2.08 V).

Conclusions

H_2(anthraphen) (**1**), a novel bis-1-hydroxy-9,10-anthraquinone-imine-type non-innocent chromophore ligand with a manifold of fully reversible redox properties, has been developed. It has a distinct coordination capacity for four equatorial positions in square planar, tetragonal pyramidal, or octahedral complexes without showing the enhanced backbone flexibility of related $N_2O_2^{2-}$ ligands such as H_2(salen) and H_2(salphen). In its coordination chemistry, high molar extinction coefficients, and electrochemical properties, **1** seems to be more related to the huge class of phthalocyanines (26000 publications to date). The protonated ligand **1**, the potassium salt **2**, and 10 3d, 4d, and 5d transition-metal complexes, namely Ti^{IV} (**3**), V^{IV} (**4**), Fe^{II} (**5**), Fe^{III} (**6**), Co^{II} (**7**), Ni^{II} (**8**), Cu^{II} (**9**), Pd^{II} (**10**), Pt^{II} (**11**), and Zn^{II} (**12**), have been characterized by NMR, UV/Vis, and IR spectroscopy, cyclic voltammetry, elemental analysis, and single-crystal XRD. The optical analysis of ligand **1** revealed extinction coefficients of up to 47000 L mol^{-1} cm^{-1} (at 252 nm) and absorption bands up to 500 nm, whereas the corresponding complexes show higher extinction coefficients and a broader absorption spectrum in the lower-energy range of visible light, for example, molar extinction coefficients of up to 66400 L mol^{-1} cm^{-1} (at 250 nm) in

the case of [V(anthraphen)O] (**4**) and broadening of the absorption spectrum in the visible-light region with a maximum at 619 nm in case of [Pd(anthraphen)] (**10**). Ligand **1** shows four reversible reduction processes in cyclic voltammetry measurements, whereas some of its complexes show five reversible oxidation and reduction events, including metal-centered redox activity. The comparison with salphen-type complexes showed that H_2(anthraphen) (**1**) and its complexes **2**–**12** have much higher molar extinction coefficients and greater stability with respect to multiple electron uptake. The simple modular synthetic approach followed in this work allows for the design of numerous variants of this chelating anthraquinone imine ligand motif. Theoretical calculations, EPR spectroscopy, and spectroelectrochemical studies will contribute to the tuning and understanding of the complex absorption behavior of this interesting class of new chromophore complexes. We believe that metal complexes of this ligand motif will be further investigated as effective redox, electro-, and Lewis acid catalysts, as biomimetic models for metalloenzymes, as "black dye" sensitizers for wide-band-gap semiconductors, for example, in dye-sensitized solar cells, as well as for other optoelectronic applications.

Experimental Section

General: All reactions, with the exception of the synthesis of 1-acetoxy-9,10-anthraquinone (**17**), were carried out under an inert atmosphere using standard Schlenk and glovebox techniques. Chemicals were used as received unless stated otherwise. All solvents were dried and purified according to common procedures and stored over 3 or 4 Å molecular sieves.[65] [Fe(hmds)$_2$(thf)],[66] [Co(hmds)$_2$(thf)],[67] [{PtCl(C$_2$H$_4$)}(μ-Cl)]$_2$,[68] [Zn(hmds)$_2$],[69] and K(hmds) were synthesized according to literature procedures. It should be mentioned that H_2(anthraphen) (**1**) never completely dissolved in the corresponding solvent in complexation reactions because of its low solubility. The anthraquinones and anthrones are numbered according to IUPAC rules. TLC plates from Merck KGaA with silica gel 60 on aluminium with fluorescence quenching F254 at room temperature were used for TLC. NMR spectra were recorded in automation or by the service department (FB Chemie, Philipps Universität Marburg) with a Bruker Avance 300, 400, or 500 spectrometer at 25 °C using CD_2Cl_2 or $CDCl_3$ as solvent and for calibration.[70] ESI and APCI high-resolution mass spectra were recorded by the service department (FB Chemie, Philipps Universität Marburg) with a Finnigan LTQ-FT spectrometer using methanol or dichloromethane as solvent. The *m/z* values are given together with their relative intensities. IR spectra were recorded with a Bruker Alpha FT-IR spectrometer with Platinum ATR sampling. Elemental analyses were performed by the service department (FB Chemie, Philipps Universität Marburg) with an Elementar vario MICRO CUBE instrument. TGA and DSC measurements were carried out with a Netzsch STA 409 CD instrument in aluminium oxide crucibles at a heating rate of 5 K min^{-1} and an argon flow rate of 40 mL min^{-1}. TGA decomposition points are given as the onset temperature and DSC data are given as the peak value. Single-crystal structure determination was performed by XRD by the service department (FB Chemie, Philipps Universität Marburg) with a Bruker D8 Quest or Stoe IPDS-II diffractometer at 100 K using Mo-K_α radiation (λ = 0.71073 Å). Stoe (X-AREA, X-RED) or Bruker (Instrument Service, APEX2, SAINT) software were used for data collection, cell refinement, and data reduction.[71,72] The WinGX[73] program suite using SIR-97[74] or SHELXT-2014[75] was used for structure solution, SHELXL-2014[75] for refinement, and Platon[76] for final validation. Absorption corrections (multiscan) were either applied within WinGX[77] or beforehand within the APEX2 software.[78] Graphics were created with Diamond 3[79] and the ellipsoids are shown at the 50 % probability level. Hydrogen atoms were constrained to the parent site if carbon-bonded and independently isotropically refined if located in the Fourier map and oxygen-bonded. For clarity, hydrogen atoms are only shown if oxygen-bonded. CCDC 1423992 (for **6**), 1423993 (for **12**), 1423994 (for **8**), 1423995 (for **11**), 1423996 (for **10**), 1423997 (for **7**), 1423998 (for **4**), 1423999 (for **1**), and 1424000 (for **9**) contain the supplementary crystallographic data for this paper. These data can be obtained free of charge from The Cambridge Crystallographic Data Centre. UV/Vis spectra were recorded with an AvaLight-DHc light source and an AvaSpec-2048 detector using fused quartz cuvettes and dichloromethane as solvent. The ligand **1** and cobalt and nickel complexes **7** and **8**, respectively, were additionally analyzed in tetrahydrofuran, and identical spectra were obtained. UV/Vis spectra were recorded for all compounds at different concentrations in the range of 5 to 20 μmol L^{-1} to calculate their molar extinction coefficients by using the Beer–Lambert law. Cyclic voltammetry was carried out with an Ivium Technologies Iviumstat or a Metrohm Autolab PGSTAT204 instrument using a RHD Instruments microcell HC under nitrogen at 25 °C. A glassy carbon working electrode (diameter d = 3 mm) and a platinum counter electrode were used. The measurements were carried out against a platinum pseudo-electrode or a silver/silver sulfide reference electrode and were calibrated by adding ferrocene as an internal standard after recording the first series of CVs. Dimethyl sulfoxide (≥99.9 %) from Sigma–Aldrich was used as solvent and was stored over 4 Å molecular sieves and distilled before use. Tetrabutylammonium hexafluorophosphate (TBAPF$_6$; ≥99.0 %) from Fluka was used as electrolyte for electrochemical analysis. All measurements were carried out at a concentration of 50 mmol L^{-1} of electrolyte and 5–10 mmol L^{-1} of sample.

1-Acetoxy-9,10-anthraquinone (17): A suspension of 1-hydroxy-9,10-anthraquinone (**16**; 12.3 g, 54.9 mmol) and sodium acetate (50.2 mg, 0.612 mmol) in acetic anhydride (80.0 mL, 846 mmol) was heated at reflux for 16 h. The orange reaction mixture was quenched with distilled water (300 mL) and stirred for 5 min at room temperature. The precipitate was filtered off, washed with distilled water (3 × 30 mL), and dried in vacuo. 1-Acetoxy-9,10-anthraquinone (**17**; 14.3 g, 98 %) was obtained as a yellow solid. R_f = 0.39 (*n*-pentane/ethyl acetate, 20:1). ^{1}H NMR ($CDCl_3$, TMS, 300 MHz; pt: pseudo triplet): δ = 8.27 (dd, $^3J_{H,H}$ = 7.8, $^4J_{H,H}$ = 1.4 Hz, 1 H, 4-H), 8.24–8.19 (m, 2 H, 5-H, 8-H), 7.78 (pt, $^3J_{H,H}$ = 7.9 Hz, 1 H, 3-H), 7.77–7.74 (m, 2 H, 7-H, 6-H), 7.41 (dd, $^3J_{H,H}$ = 8.0, $^4J_{H,H}$ = 1.3 Hz, 1 H, 2-H), 2.49 (s, 3 H, 12-H) ppm. ^{13}C NMR ($CDCl_3$, TMS, 75 MHz): δ = 182.5 (C-10), 181.9 (C-9), 169.7 (C-11), 150.4 (C-1), 135.4 (C-4a), 135.0 (C-3), 134.4 (C-7), 134.2 (C-8a), 134.1 (C-6), 132.8 (C-5a), 130.0 (C-2), 127.3 (C-8), 127.1 (C-5), 125.9 (C-4), 125.0 (C-1a), 21.3 (C-12) ppm. IR (neat): $\tilde{\nu}$ = 2361 (w), 1764 (s, C=O) 1672 (s, C=O), 1589 (m), 1442 (w), 1362 (w), 1323 (m), 1278 (s), 1239 (w), 1182 (s), 1165 (m, C–O), 1041 (w), 1020 (w), 995 (w), 970 (w), 899 (m), 861 (m), 808 (s), 777 (w), 731 (m), 704 (s), 688 (s), 652 (m), 582 (m), 543 (m), 530 (m), 483 (m), 452 (w), 410 (w) cm^{-1}. MS (ESI+, CH_2Cl_2): *m/z* (%) = 289.1 (100). HRMS: calcd. for [M + Na]$^+$ 289.0471; found 289.0471. $C_{16}H_{10}O_4$ (266.25): calcd. C72.18, H 3.79; found C 72.23, H 3.71.

1-Hydroxy-9,9-dimethoxy-10-anthrone (18): A solution of sodium methoxide (4.64 g, 85.9 mmol) in methanol (40 mL) was slowly added to a suspension of 1-acetoxy-9,10-anthraquinone (**17**; 6.50 g, 24.4 mmol) in tetrahydrofuran (210 mL) and the resulting mixture was stirred for 30 min at room temperature. The dark-red reaction mixture was quenched with distilled water (280 mL) and

acetic acid was added until the color changed to yellow. Afterwards, distilled water (560 mL) was added and the yellow precipitate was filtered off and washed with distilled water (3 × 100 mL). The raw product was purified by column chromatography [deactivated (triethylamine/*n*-pentane) silica gel; *n*-pentane/ethyl acetate, 20:1] and dried in vacuo. 1-Hydroxy-9,9-dimethoxy-10-anthrone (**18**; 4.57 g, 69 %) was obtained as a yellow solid. R_f = 0.48 (*n*-pentane/ethyl acetate, 20:1). ^{1}H NMR (CD_2Cl_2, TMS, 300 MHz; pt: pseudo triplet): δ = 8.27 (dd, $^3J_{H,H}$ = 7.9, $^4J_{H,H}$ = 0.9 Hz, 1 H, 5-H), 8.03 (s, 1 H, OH), 7.85 (dd, $^3J_{H,H}$ = 7.8, $^4J_{H,H}$ = 1.2 Hz, 1 H, 4-H), 7.84 (dd, $^3J_{H,H}$ = 7.7, $^4J_{H,H}$ = 1.1 Hz, 1 H, 8-H), 7.79 (ddd, $^3J_{H,H}$ = 7.8, 7.2, $^4J_{H,H}$ = 1.4 Hz, 1 H, 7-H), 7.62 (ddd, $^3J_{H,H}$ = 7.9, 7.2, $^4J_{H,H}$ = 1.4 Hz, 1 H, 6-H), 7.49 (pt, $^3J_{H,H}$ = 7.9 Hz, 1 H, 3-H), 7.21 (dd, $^3J_{H,H}$ = 8.1, $^4J_{H,H}$ = 1.1 Hz, 1 H, 2-H), 2.96 (s, 6 H, 2 OCH_3) ppm. ^{13}C NMR (CD_2Cl_2, TMS, 75 MHz): δ = 182.4 (C-10), 156.4 (C-1), 138.6 (C-8a), 134.8 (C-4a), 134.7 (C-7), 133.8 (C-5a), 131.6 (C-3), 130.4 (C-6), 127.3 (C-5), 127.1 (C-8), 122.6 (C-2, C-1a), 119.3 (C-4), 100.2 (C-9), 52.3 (2 OCH_3) ppm. IR: $\tilde{\nu}$ = 3393 (w, br), 2998 (w), 2931 (w), 2828 (w), 1671 (m), 1638 (w), 1593 (m), 1452 (m), 1317 (m), 1272 (s), 1252 (s), 1223 (m), 1199 (m), 1157 (m), 1065 (s), 998 (s), 872 (m), 830 (w), 767 (s), 707 (m) cm^{-1}. MS (ESI+, CH_3OH): *m/z* (%) = 293.1 (100). HRMS: calcd. for $[M + Na]^+$ 293.0784; found 293.0788.

H_2(anthraphen) (1): A solution of 1-hydroxy-9,9-dimethoxy-10-anthrone (**18**; 8.37 g, 31.0 mmol) and *o*-phenylenediamine (1.68 g, 15.5 mmol) in toluene (250 mL) was heated at reflux for 24 h, cooled to –30 °C, and filtered. The solid was washed with cold toluene (2 × 20 mL) and purified by column chromatography (silica gel, $CHCl_3$). H_2(anthraphen) (**1**; 5.85 g, 72 %) was obtained as a red solid. R_f = 0.18 ($CHCl_3$). ^{1}H NMR ($CDCl_3$, TMS, 300 MHz; pt: pseudo triplet): δ = 13.40 (s, 2 H, OH), 8.08 (dd, $^3J_{H,H}$ = 8.2, $^4J_{H,H}$ = 1.5 Hz, 2 H, 5-H, 15-H), 7.63–7.58 (m, 6 H, 4-H, 14-H, 6-H, 16-H, 8-H, 18-H), 7.46 (pt, $^3J_{H,H}$ = 7.92 Hz, 2 H, 3-H, 13-H), 7.39–7.34 (m, 4 H, 7-H, 17-H, 23-H, 26-H), 7.28–7.23 (m, 2 H, 24-H, 25-H), 7.03 (dd, $^3J_{H,H}$ = 8.2, $^4J_{H,H}$ = 1.1 Hz, 2 H, 2-H/, 12-H) ppm. ^{13}C NMR ($CDCl_3$, TMS, 75 MHz): δ = 181.5 (C-10, C-20), 162.1 (C-9, C-19), 161.0 (C-1, C-11), 136.6 (C-21, C-22), 133.8 (C-3, C-13), 132.9 (C-6, C-16), 132.7 (C-5a, C-15a), 132.6 (C-7, C-17), 131.6 (C-4a, C-14a), 130.1 (C-8a, C-18a), 128.0 (C-5, C-15), 127.3 (C-8, C-18), 126.9 (C-23, C-26), 123.8 (C-2, C-12), 122.5 (C-24, C-25), 118.9 (C-4, C-14), 117.7 (C-1a, C-11a) ppm. IR: $\tilde{\nu}$ = 1665 (s), 1588 (s), 1552 (m), 1487 (m), 1450 (s), 1344 (m), 1318 (m), 1288 (s), 1270 (s), 1225 (s), 1155 (m), 1143 (m), 1111 (m), 1094 (w), 1069 (w), 1047 (w), 1035 (w), 1014 (m), 963 (w), 882 (m), 848 (m), 829 (m), 784 (s), 776 (s), 765 (s), 726 (w), 709 (s), 697 (s), 656 (m), 618 (w), 553 (w), 536 (w), 524 (w), 488 (w), 470 (m), 435 (w) cm^{-1}. MS (APCI+, CH_3OH): *m/z* (%) = 521.3 (100). HRMS: calcd. for $[M + H]^+$ 521.1496; found 521.1496. $C_{34}H_{20}N_2O_4$ (520.53): calcd. C 78.45, H 3.87, N 5.38; found C 78.21, H 3.92, N 5.20. TGA: 297 °C (decomp.); DSC: 296 (endoth.), 300 (exoth.) °C.

[K_2(anthraphen)(thf)$_2$] (2): A suspension of potassium hydride (7.7 mg, 0.019 mmol) in tetrahydrofuran (2 mL) was added to a suspension of H_2(anthraphen) (**1**; 50 mg, 0.096 mmol) in tetrahydrofuran, (8 mL) and the resulting mixture was stirred for 1 h at room temperature. After concentrating the solution to a few milliliters, the precipitate was filtered off and washed with tetrahydrofuran (2 × 2 mL). [K_2(anthraphen)]•THF (**2**; 33 mg, 58 %) was obtained as a violet-black solid. IR: $\tilde{\nu}$ = 2962 (w, br), 1645 (m), 1586 (w), 1566 (m), 1515 (m), 1449 (m), 1409 (m), 1369 (w), 1336 (w), 1296 (m), 1258 (s), 1207 (w), 1154 (w), 1089 (m), 1016 (s br), 921 (w), 883 (m), 796 (s), 774 (s), 748 (m), 705 (s), 661 (m), 615 (w), 597 (w), 547 (w), 529 (w), 513 (w), 469 (w), 446 (w), 435 (w) cm^{-1}. $C_{34}H_{18}K_2N_2O_4$•$2C_4H_8O$ (668.82): calcd. C 68.08, H 4.63, N 3.78; found C 68.01, H 4.66, N 4.21.

[Ti(anthraphen)(NMe_2)$_2$] (3): Tetrakis(dimethylamido)titanium (50.0 µL, 0.214 mmol) was added to a suspension of H_2(anthraphen) (**1**; 104 mg, 0.201 mmol) in toluene (18 mL) and the resulting mixture was heated at reflux for 30 min. All the volatile components were removed in vacuo. [Ti(anthraphen)(NMe_2)$_2$] (**3**; 112 mg, 86 %) was obtained as a green-black solid. ^{1}H NMR (CD_2Cl_2, TMS, 300 MHz; pt: pseudo triplet): δ = 8.31 (d, $^3J_{H,H}$ = 8.5 Hz, 2 H, H_{ar}), 7.95 (d, $^3J_{H,H}$ = 8.9 Hz, 2 H, H_{ar}), 7.90 (dd, $^3J_{H,H}$ = 8.9, $^4J_{H,H}$ = 1.1 Hz, 2 H, H_{ar}), 7.41 (pt, $^3J_{H,H}$ = 7.9 Hz, 2 H, H_{ar}), 7.27–7.14 (m, 4 H, H_{ar}), 6.76 (dd, $^3J_{H,H}$ = 7.2, $^4J_{H,H}$ = 0.9 Hz, 2 H, H_{ar}), 6.24 (dd, $^3J_{H,H}$ = 6.0, $^4J_{H,H}$ = 3.4 Hz, 2 H, H_{ar}), 6.24 (dd, $^3J_{H,H}$ = 5.9, $^4J_{H,H}$ = 3.4 Hz, 2 H, H_{ar}), 3.30 [s, 12 H, 2 $N(CH_3)_2$] ppm. ^{13}C NMR: too poorly soluble in common solvents. IR: $\tilde{\nu}$ = 2839 (w, br), 2766 (w, br), 1580 (w), 1547 (w), 1512 (w), 1461 (m), 1438 (m), 1370 (s), 1300 (s), 1250 (s), 1185 (w), 1151 (w), 1115 (w), 1055 (w), 1024 (m), 1004 (s), 646 (w), 756 (m), 729 (m), 713 (m), 687 (m), 663 (m), 645 (m), 609 (m), 576 (m), 553 (m) cm^{-1}. MS (APCI+, CH_3OH): *m/z* (%) = 597.2 (25). HRMS: calcd. for $[C_{34}H_{18}N_2O_4Ti + CH_3O]^+$ 597.0928; found 597.0922.

[V(anthraphen)O] (4): A suspension of H_2(anthraphen) (**1**; 98 mg, 0.19 mmol) and vanadyl acetylacetonate (52 mg, 0.20 mmol) in toluene (15 mL) was heated at reflux for 18 h. Afterwards, the reaction mixture was filtered, washed with toluene (2 × 2 mL), and dried in vacuo. [V(Anthraphen)O] (**4**; 94 mg, 86 %) was obtained as a red solid. IR: $\tilde{\nu}$ = 1666 (s), 1581 (s), 1553 (w), 1504 (s), 1472 (w), 1452 (w), 1415 (m), 1361 (m), 1339 (w), 1305 (m), 1265 (s), 1242 (m), 1222 (m), 1157 (m), 1145 (w), 1024 (w), 978 (s), 894 (m), 831 (m), 799 (w), 779 (m), 748 (m), 712 (s), 703 (s), 662 (w), 543 (m) cm^{-1}. MS (APCI+, CH_3OH): *m/z* (%) = 585.3 (50), 586.3 (100). HRMS: calcd. for $[M]^+$ 585.0650; found 585.0649; calcd. for $[M + H]^+$ 586.0728; found 586.0731. $C_{34}H_{18}N_2O_5V$ (585.46): calcd. C 69.75, H 3.10, N 4.78; found C 69.04, H 3.01, N 5.15.

[Fe(anthraphen)] (5): A solution of [Fe(hmds)$_2$(thf)] (159 mg, 0.354) in tetrahydrofuran (10 mL) was added to a suspension of H_2(anthraphen) (**1**; 183 mg, 0.352 mmol) in tetrahydrofuran (20 mL) and the resulting mixture was heated at reflux for 30 min. The reaction mixture was filtered, washed with hot *n*-hexane, and dried in vacuo. [Fe(anthraphen)] (**5**; 189 mg, 93 %) was obtained as a black solid. IR: $\tilde{\nu}$ = 1657 (s), 1616 (m), 1567 (s), 1531 (m), 1472 (s), 1427 (w), 1413 (m), 1351 (s), 1301 (s), 1261 (s), 1238 (w), 1218 (s), 1152 (m), 1139 (w), 1107 (w), 1072 (w), 1041 (w), 1022 (m), 930 (w), 883 (m), 826 (m), 791 (m), 770 (s), 740 (s), 706 (s), 663 (w), 651 (w), 633 (w), 610 (w), 497 (m) cm^{-1}. MS (APCI+, CH_3OH): *m/z* (%) = 574.1 (100), 605.4 (75). HRMS: calcd. for $[M]^+$ 574.0611; found 574.0610; calcd. for $[M + CH_3OH]^+$ 606.0872; found 606.0869. $C_{34}H_{18}N_2O_4Fe$•C_4H_8O (646.47): calcd. C 70.60, H 4.05, N 4.33; found C 70.65, H 4.21, N 4.45.

[Fe(anthraphen)Cl] (6): A solution of K(hmds) (103 mg, 0.516 mmol) in toluene (5 mL) was added to a suspension of H_2 (anthraphen) (**1**; 126 mg, 0.242 mmol) in toluene (10 mL) and the resulting mixture was heated at reflux for 30 min. The dark-red precipitate was filtered, washed with toluene (2 × 10 mL), and suspended in tetrahydrofuran (20 mL). A solution of $FeCl_3$ (39 mg, 0.24 mmol) in tetrahydrofuran (5 mL) was added and the resulting suspension was heated at reflux for 1 h. The reaction mixture was concentrated to a few milliliters and then *n*-pentane was added until precipitation occurred. The precipitate was filtered off, washed with methanol (2 × 5 mL), and dried in vacuo. [Fe(anthraphen)Cl] (**6**; 107 mg, 72 %) was obtained as a brown-black solid. IR: $\tilde{\nu}$ = 1665 (s), 1581 (s), 1510 (s), 1472 (w), 1446 (w), 1418 (w), 1301 (s), 1264 (s), 1241 (m), 1225 (m), 1158 (w), 1143 (w), 1108 (w), 1074 (w), 1044 (w), 1021 (m), 892 (m), 829 (m), 777 (m), 751 (m), 735 (m), 709 (s), 662 (w), 548 (w), 498 (w) cm^{-1}. MS (APCI+, CH_2Cl_2): *m/z* (%) = 574.2

(100). HRMS: calcd. for [M – Cl]$^+$ 574.0611; found 574.0606. $C_{34}H_{18}N_2O_4FeCl{\cdot}0.5C_4H_8O$ (645.87): calcd. C 66.95, H 3.43, N 4.34; found C 66.92, H 3.45, N 4.37.

[Co(anthraphen)] (7): A solution of [Co(hmds)$_2$(thf)] (93 mg, 0.24 mmol) in toluene (9 mL) was added to a suspension of H_2(anthraphen) (**1**; 121 mg, 0.233 mmol) in toluene (15 mL) and the resulting mixture was heated at reflux for 2.5 h. The reaction mixture was filtered, washed with cold toluene (2 × 3 mL), and dried in vacuo. [Co(anthraphen)] (**7**; 122 mg, 91 %) was obtained as a black solid. IR: $\tilde{\nu}$ = 1663 (m), 1645 (s), 1578 (s), 1536 (w), 1480 (m), 1466 (m), 1448 (w), 1407 (m), 1369 (m), 1350 (m), 1327 (w), 1302 (s), 1266 (s), 1242 (m), 1230 (m), 1183 (w), 1170 (w), 1154 (m), 1143 (m), 1111 (w), 1075 (w), 1027 (w), 983 (w), 965 (w), 945 (w), 893 (w), 883 (w), 825 (w), 809 (w), 777 (s), 761 (s), 734 (s), 717 (w), 701 (s), 662 (w), 651 (w), 620 (w), 591 (w), 561 (w), 545 (w), 534 (w), 514 (w), 465 (w), 432 (w) cm^{-1}. MS (APCI+, CH_2Cl_2): *m/z* (%) = 578.17 (100). HRMS: calcd. for [M + H]$^+$ 578.0671; found 578.0672. $C_{34}H_{18}N_2O_4Co{\cdot}C_7H_8$ (668.58): calcd. C 73.54, H 3.91, N 4.18, Co 8.80; found C 73.84, H 3.82, N 4.77, Co 8.53.

[Ni(anthraphen)] (8): A solution of [Ni(OAc)$_2$·4H$_2$O] (99 mg, 0.40 mmol) in methanol (4 mL) was added to a suspension of H_2(anthraphen) (**1**; 189 mg, 0.363 mmol) in methanol (20 mL) and the resulting mixture was heated at reflux for 3.5 h. The reaction mixture was filtered at +4 °C, washed with cold methanol, and dried in vacuo. [Ni(anthraphen)] (**8**; 185 mg, 88 %) was obtained as a black solid. ^{1}H NMR (CD_2Cl_2, TMS, 300 MHz): δ = 8.27 (dd, $^3J_{H,H}$ = 7.8, $^4J_{H,H}$ = 1.2 Hz, 2 H, 5-H, 15-H), 8.01 (d, $^3J_{H,H}$ = 7.7 Hz, 2 H, 8-H, 18-H), 7.72 (ddd, $^3J_{H,H}$ = 7.7, 7.4, $^4J_{H,H}$ = 1.1 Hz, 2 H, 6-H, 16-H), 7.69 (dd, $^3J_{H,H}$ = 7.0, $^4J_{H,H}$ = 1.2 Hz, 2 H, 4-H, 14-H), 7.58 (ddd, $^3J_{H,H}$ = 8.1, 7.3, $^4J_{H,H}$ = 1.5 Hz, 2 H, 7-H, 17-H), 7.44 (dd, $^3J_{H,H}$ = 8.6, 7.1 Hz, 2 H, 3-H, 13-H), 7.32 (dd, $^3J_{H,H}$ = 8.6, $^4J_{H,H}$ = 1.3 Hz, 2 H, 2-H, 12-H), 6.73–6.68 (m, 2 H, 24-H, 25-H), 6.64–6.59 (m, 2 H, 23-H, 26-H) ppm. ^{13}C NMR (CD_2Cl_2, TMS, 75 MHz): δ = 183.4 (C-10, C-20), 165.2 (C-1, C-11), 162.5 (C-9, C-19), 148.1 (C-21, C-22), 134.0 (C-5a, C-15a), 133.9 (C-3, C-13), 133.0 (C-6, C-16), 132.3 (C-7, C-17), 132.0 (C-8a, C-18a), 131.8 (C-4a, C-14a), 131.3 (C-8, C-18), 129.5 (C-2, C-12), 128.2 (C-5, C-15), 126.0 (C-23, C-26), 124.8 (C-24, C-25), 122.2 (C-1a, C-11a), 118.2 (C-4, C-14) ppm. IR: $\tilde{\nu}$ = 1651 (m), 1579 (s), 1492 (m), 1468 (m), 1450 (w), 1404 (m), 1369 (m), 1301 (s), 1264 (s), 1229 (s), 1169 (w), 1141 (m), 1076 (w), 1030 (m), 899 (w), 827 (w), 788 (w), 768 (s), 750 (w), 734 (w), 723 (w), 703 (s), 687 (w), 653 (w), 544 (w) cm^{-1}. MS (APCI+, CH_2Cl_2): *m/z* (%) = 577.2 (65). HRMS: calcd. for [M + H]$^+$ 577.0693; found 577.0693. $C_{34}H_{18}N_2O_4Ni{\cdot}CH_3OH$ (609.25): calcd. C 69.00, H 3.64, N 4.60; found C 68.85, H 3.62, N 4.64.

[Pd(anthraphen)] (9): A solution of [Pd(OAc)$_2$] (55 mg, 0.25 mmol) in methanol (5 mL) was added to a suspension of H_2(anthraphen) (**1**; 108 mg, 0.208 mmol) in tetrahydrofuran (20 mL) and the resulting mixture was heated at reflux for 3 h. The reaction mixture was filtered at +4 °C, washed with cold tetrahydrofuran, and dried in vacuo. [Pd(anthraphen)] (**9**; 121 mg, 93 %) was obtained as a green-black solid. ^{1}H NMR ($CDCl_3$, TMS, 300 MHz; pt: pseudo triplet): δ = 8.32 (d, $^3J_{H,H}$ = 7.8 Hz, 2 H, 5-H, 15-H), 7.96 (d, $^3J_{H,H}$ = 7.9 Hz, 2 H, 8-H, 18-H), 7.84 (dd, $^3J_{H,H}$ = 7.0, $^4J_{H,H}$ = 0.9 Hz, 2 H, 4-H, 14-H), 7.72 (pt, $^3J_{H,H}$ = 7.3 Hz, 2 H, 6-H, 16-H), 7.65 (dd, $^3J_{H,H}$ = 7.5, $^4J_{H,H}$ = 0.9 Hz, 2 H, 2-H, 12-H), 7.59–7.53 (m, 4 H, 7-H, 17-H, 3-H, 13-H), 6.84 (dd, $^3J_{H,H}$ = 6.3, 3.4 Hz, 2 H, 24-H, 25-H), 6.69 (dd, $^3J_{H,H}$ = 6.3, 3.4 Hz, 2 H, 23-H, 26-H) ppm. ^{13}C NMR ($CDCl_3$, TMS, 125 MHz): δ = 183.7 (C-10, C-20), 166.6 (C-1, C-11), 160.7 (C-9, C-19), 147.7 (C-21, C-22), 134.1 (C-5a, C-15a), 134.0 (C-3, C-13), 132.8 (C-6, C-16), 132.7, 132.6 (C-4a, C-14a, C-8a, C-18a), 132.1 (C-7, C-17), 131.2 (C-8, C-18), 130.3 (C-2, C-12), 128.2 (C-5, C-15), 125.9 (C-23, C-26), 125.5 (C-24, C-25), 122.5 (C-1a, C-11a), 119.3 (C-4, C-4) ppm. IR: $\tilde{\nu}$ = 1650 (m), 1578 (m), 1492 (m), 1468 (m), 1445 (w), 1399 (w), 1357 (m), 1299 (s), 1258 (s), 1236 (m), 1212 (s), 1166 (w), 1136 (m), 1076 (w), 1032 (m), 1024 (m), 969 (w), 893 (w), 825 (w), 766 (s), 731 (w), 716 (m), 702 (s), 681 (w), 652 (w), 547 (w), 525 (w), 513 (w) cm^{-1}. MS (APCI+, CH_2Cl_2): *m/z* (%) = 625.22 (85). HRMS: calcd. for [M + H]$^+$ 625.0387; found 625.0367. $C_{34}H_{18}N_2O_4Pd{\cdot}CH_3OH$ (656.98): calcd. C 63.99, H 3.38, N 4.26; found C 63.79, H 3.30, N 4.42.

[Pt(anthraphen)] (10): A suspension of H_2(anthraphen) (**1**; 150 mg, 0.288 mmol) and sodium acetate (49 mg, 0.60 mmol) in dimethylformamide (10 mL) was stirred for 15 min at room temperature. Afterwards, a solution of [{PtCl(C_2H_4)}(μ-Cl)]$_2$ (232 mg, 0.394 mmol) in dimethylformamide (10 mL) was added and the resulting suspension was heated at 110 °C for 4 d. The reaction mixture was filtered, the solvent was removed from the filtrate in vacuo, and the residue was recrystallized from chloroform. [Pt(anthraphen)] (**10**; 42 mg, 20 %) was obtained as a black solid. ^{1}H NMR ($CDCl_3$, TMS, 400 MHz; pt: pseudo triplet): δ = 8.31 (dd, $^3J_{H,H}$ = 7.6, $^4J_{H,H}$ = 1.0 Hz, 2 H, H_{Ar}), 7.96 (d, $^3J_{H,H}$ = 8.0 Hz, 2 H, H_{Ar}), 7.89 (dd, $^3J_{H,H}$ = 6.62, $^4J_{H,H}$ = 1.73 Hz, 2 H, H_{Ar}), 7.76 (pt, $^3J_{H,H}$ = 7.7 Hz, 2 H, H_{Ar}), 7.70–7.53 (m, 6 H, H_{Ar}), 6.91 (dd, $^3J_{H,H}$ = 6.6, $^4J_{H,H}$ = 3.5 Hz, 2 H, 24-H, 25-H), 6.66 (dd, $^3J_{H,H}$ = 6.4, $^4J_{H,H}$ = 3.4 Hz, 2 H, 23-H, 26-H) ppm. ^{13}C NMR ($CDCl_3$, TMS, 100 MHz): δ = 184.1 (C-10, C-20), 165.0, 157.1 (C-1, C-11, C-9, C-19), 149.1 (C-21, C-22), 133.6 (2 C_q), 133.4, 133.2, 132.5, 132.1, 131.5 (10 C_{Ar}), 130.9, 130.2 (4 C_q), 128.3 (2 C_{Ar}), 126.0 (C-23, C-26), 125.5 (C-24, C-25), 123.1 (2 C_q), 120.4 (2 C_{Ar}) ppm. IR: $\tilde{\nu}$ = 2962 (w), 2923 (w), 2852 (w), 2402 (w), 2382 (m), 2363 (w), 2350 (m), 2336 (m), 2327 (m), 2306 (w), 2293 (w), 2251 (w), 1665 (m), 1584 (m), 1493 (w), 1469 (w), 1451 (w), 1405 (w), 1366 (w), 1305 (w), 1260 (s), 1139 (w), 1092 (w), 1016 (m), 910 (w), 863 (w), 796 (s), 753 (w), 724 (m), 704 (m), 674 (s), 662 (s) cm^{-1}. MS (APCI+, CH_3OH): *m/z* (%) = 714.3 (100). HRMS: calcd. for [M + H]$^+$ 714.0990; found 714.0980.

[Cu(anthraphen)] (11): A solution of [Cu(OAc)$_2$·H$_2$O] (69 mg, 0.35 mmol) in methanol (4 mL) was added to a suspension of H_2(anthraphen) (**1**; 181 mg, 0.348 mmol) in tetrahydrofuran (20 mL) and the resulting suspension was heated at reflux for 3.5 h. The black reaction mixture was filtered at +4 °C, washed with cold methanol, and dried in vacuo. [Cu(anthraphen)] (**11**; 171 mg, 85 %) was obtained as a black solid. IR: $\tilde{\nu}$ = 1663 (m), 1581 (s), 1501 (s), 1474 (s), 1406 (s), 1355 (s), 1303 (s), 1261 (s), 1247 (s), 1220 (s), 1157 (m), 1140 (m), 1110 (m), 1073 (m), 1046 (m), 1025 (m), 888 (m), 828 (m), 801 (w), 782 (m), 772 (s), 753 (s), 741 (m), 710 (s), 696 (s), 657 (m), 543 (s), 522 (s) cm^{-1}. MS (APCI+, CH_2Cl_2): *m/z* (%) = 582.2 (100). HRMS: calcd. for [M + H]$^+$ 582.0635; found 582.0635. $C_{34}H_{18}N_2O_4Cu$ (582.06): calcd. C 70.16, H 3.12, N 4.81; found C 69.72, H 3.15, N 4.99.

[Zn(anthraphen)] (12): A solution of [Zn(hmds)$_2$] (77 mg, 0.20 mmol) in toluene (5 mL) was added to a suspension of H_2-(anthraphen) (**1**; 100 mg, 0.192 mmol) in toluene (15 mL) and the resulting suspension was heated at reflux for 1.5 h. The reaction mixture was filtered at +4 °C, washed with cold toluene, and dried in vacuo. [Zn(anthraphen)] (**12**; 70 mg, 62 %) was obtained as a dark-red solid. ^{1}H NMR ($CDCl_3$+C_5D_5N, TMS, 300 MHz; pt: pseudo triplet): δ = 8.24 (dd, $^3J_{H,H}$ = 7.7, $^4J_{H,H}$ = 0.8 Hz, 2 H, 5-H, 15-H), 7.65 (d, $^3J_{H,H}$ = 7.6 Hz, 2 H, 8-H, 18-H), 7.58 (pt, $^3J_{H,H}$ = 7.5 Hz, 2 H, 6-H, 16-H), 7.49 (dd, $^3J_{H,H}$ = 5.9, $^4J_{H,H}$ = 2.6 Hz, 2 H, 4-H, 14-H), 7.44 (dpt, $^3J_{H,H}$ = 7.88, $^4J_{H,H}$ = 1.2 Hz, 2 H, 7-H, 17-H), 7.38–7.31 (m, 4 H, 2-H, 12-H, 3-H, 13-H), 6.76 (dd, $^3J_{H,H}$ = 6.1, $^4J_{H,H}$ = 3.4 Hz, 2 H, 24-H, 25-H), 6.52 (dd, $^3J_{H,H}$ = 6.1, $^4J_{H,H}$ = 3.4 Hz, 2 H, 23-H, 26-H) ppm. ^{13}C NMR ($CDCl_3$+C_5D_5N, TMS, 75 MHz): δ = 185.2 (C-10, C-20), 170.5 (C-1, C-11), 165.9 (C-9, C-19), 141.7 (C-21, C-22), 134.7 (C-5a, C-15a), 133.3 (C-4a, C-14a), 133.2 (C-3, C-13), 132.6 (C-8a, C-18a), 131.7 (C-2, C-12), 131.5 (C-6, C-16), 131.2 (C-7, C-17), 129.3 (C-8, C-18), 127.7

(C-5, C-15), 126.2 (C-24, C-25), 123.8 (C-23, C-26), 119.7 (C-1a, C-11a), 115.4 (C-4, C-14) ppm. IR: $\tilde{\nu}$ = 1662 (s), 1581 (s), 1558 (m), 1521 (s), 1474 (w), 1446 (w), 1417 (m), 1356 (w), 1343 (m), 1322 (m), 1296 (s), 1258 (s), 1243 (m), 1220 (m), 1188 (w), 1164 (m), 1142 (m), 1111 (w), 1071 (w), 1043 (w), 1020 (w), 887 (m), 830 (w), 792 (m), 776 (m), 751 (s), 731 (w), 709 (s), 692 (w), 674 (w), 663 (m), 601 (w), 561 (w), 540 (m), 518 (w), 499 (w), 463 (w) cm^{-1}. MS (APCI–, CH_2Cl_2): *m/z* (%) = 617.31 (30). HRMS: calcd. for $[M + Cl]^-$ 617.0252; found 617.0249. $C_{34}H_{18}N_2O_4Zn$ (583.90): calcd. C 69.94, H 3.11, N 4.80; found C 69.86, H 3.25, N 4.76.

Acknowledgments

This work was supported by the Deutsche Forschungsgemeinschaft (DFG) within the graduate school "Functionalization of Semiconductors" (GRK 1782).

Keywords: N,O ligands · Schiff bases · Transition metals · Ligand design · Chromophores

[1] H. Schiff, *Ann. Chem. Pharm.* **1864**, *131*, 118–119.
[2] P. A. Vigato, S. Tamburini, *Coord. Chem. Rev.* **2004**, *248*, 1717–2128.
[3] F. Bedioui, *Coord. Chem. Rev.* **1995**, *144*, 39–68.
[4] R. Drozdzak, B. Allaert, N. Ledoux, I. Dragutan, V. Dragutan, F. Verpoort, *Coord. Chem. Rev.* **2005**, *249*, 3055–3074.
[5] C. Ettling, *Ann. Chem. Pharm.* **1840**, *35*, 241–276.
[6] M. D. Hobday, T. D. Smith, *Coord. Chem. Rev.* **1972**, *9*, 311–337.
[7] P. Pfeiffer, E. Breith, E. Lübbe, T. Tsumaki, *Justus Liebigs Ann. Chem.* **1933**, *503*, 84–130.
[8] P. G. Cozzi, *Chem. Soc. Rev.* **2004**, *33*, 410–421.
[9] T. Katsuki, *J. Mol. Catal. A* **1996**, *113*, 87–107.
[10] E. M. McGarrigle, D. G. Gilheany, *Chem. Rev.* **2005**, *105*, 1563–1602.
[11] E. N. Jacobsen, *Acc. Chem. Res.* **2000**, *33*, 421–431.
[12] M. Tokunaga, J. F. Larrow, F. Kakiuchi, E. N. Jacobsen, *Science* **1997**, *277*, 936–938.
[13] D. J. Darensbourg, *Chem. Rev.* **2007**, *107*, 2388–2410.
[14] A. Decortes, A. M. Castilla, A. W. Kleij, *Angew. Chem. Int. Ed.* **2010**, *49*, 9822–9837; *Angew. Chem.* **2010**, *122*, 10016.
[15] Y. Shimazaki, D. P. Stack, T. Storr, *Inorg. Chem.* **2009**, *48*, 8383–8392.
[16] O. Rotthaus, O. Jarjayes, C. Philouze, C. P. D. Valle, F. Thomas, *Dalton Trans.* **2009**, 1792–1800.
[17] T. Storr, P. Verma, Y. Shimazaki, E. C. Wasinger, T. D. P. Stack, *Chem. Eur. J.* **2010**, *16*, 8980–8983.
[18] T. Storr, P. Verma, R. C. Pratt, E. C. Wasinger, Y. Shimazaki, T. D. P. Stack, *J. Am. Chem. Soc.* **2008**, *130*, 15448–15459.
[19] T. Storr, E. C. Wasinger, R. C. Pratt, T. D. P. Stack, *Angew. Chem. Int. Ed.* **2007**, *46*, 5198–5201; *Angew. Chem.* **2007**, *119*, 5290.
[20] O. Rotthaus, O. Jarjayes, F. Thomas, C. Philouze, C. P. D. Valle, E. Saint-Aman, J.-L. Pierre, *Chem. Eur. J.* **2006**, *12*, 2293–2302.
[21] Y. Shimazaki, F. Tani, K. Fukui, Y. Naruta, O. Yamauchi, *J. Am. Chem. Soc.* **2003**, *125*, 10512–10513.
[22] M. M. Khusniyarov, E. Bill, T. Weyhermüller, E. Bothe, K. Harms, J. Sundermeyer, L. Wieghardt, *Chem. Eur. J.* **2008**, *14*, 7608–7622.
[23] a) B. A. Jazdzewski, W. B. Tolman, *Coord. Chem. Rev.* **2000**, *200–202*, 633–685; b) G. H. Loew, D. L. Harris, *Chem. Rev.* **2000**, *100*, 407–419.
[24] a) V. Lyaskovskyy, B. de Bruin, *ACS Catal.* **2012**, *2*, 270–279; b) O. R. Luca, R. H. Crabtree, *Chem. Soc. Rev.* **2013**, *42*, 1440–1459.
[25] C. G. Pierpont, *Coord. Chem. Rev.* **2001**, *216–217*, 99–125.
[26] P. Verma, J. Weir, L. Mirica, T. D. P. Stack, *Inorg. Chem.* **2011**, *50*, 9816–9825.
[27] K. Ray, T. Petrenko, K. Wieghardt, F. Neese, *Dalton Trans.* **2007**, 1552–1566.
[28] D. Schweinfurth, F. Weisser, B. Sarkar, *Nachr. Chem.* **2009**, *57*, 862–866.
[29] W. Kaim, *Coord. Chem. Rev.* **2011**, *255*, 2503–2513.
[30] W. Kaim, B. Schwederski, *Coord. Chem. Rev.* **2010**, *254*, 1580–1588.
[31] W. Kaim, *Eur. J. Inorg. Chem.* **2012**, 343–348.
[32] W. Kaim, *Inorg. Chem.* **2011**, *50*, 9752–9765.
[33] A. Vlcek Jr., *Coord. Chem. Rev.* **2002**, *230*, 225–242.
[34] M. M. Khusniyarov, K. Harms, O. Burghaus, J. Sundermeyer, B. Sarkar, W. Kaim, J. van Slageren, C. Duboc, J. Fiedler, *Dalton Trans.* **2008**, 1355–1365.
[35] O. Siri, P. Braunstein, *Chem. Commun.* **2000**, 2223–2224.
[36] Q.-Z. Yang, O. Siri, P. Braunstein, *Chem. Commun.* **2005**, 2660–2662.
[37] B. Sarkar, S. Schweinfurth, N. Deibel, F. Weisser, *Coord. Chem. Rev.* **2015**, *293*, 250–262.
[38] C. G. Pierpont, C. W. Lange, *Prog. Inorg. Chem.* **1994**, *41*, 381–492.
[39] H. Chun, T. Weyhermüller, E. Bill, K. Wieghardt, *Angew. Chem. Int. Ed.* **2001**, *40*, 2489–2492; *Angew. Chem.* **2001**, *113*, 2552.
[40] A. A. Kutyrev, S. J. Fomin, V. V. Moskva, *Russ. J. Gen. Chem.* **1996**, *66*, 776–783.
[41] T. V. Kharlamova, *Chem. Nat. Compd.* **2009**, *45*, 629–633.
[42] S. I. Popov, V. P. Volosenko, *Russ. J. Org. Chem.* **1982**, *18*, 145–149.
[43] T. Tsuchiya, S. Ohmuro, *Tetrahedron Lett.* **2002**, *43*, 611–615.
[44] V. P. Volosenko, S. I. Popov, *Russ. J. Org. Chem.* **1981**, *17*, 874–875.
[45] A. A. Kutyrev, S. J. Fomin, V. V. Moskva, *Russ. J. Gen. Chem.* **1996**, *66*, 757–764.
[46] N. B. Pahor, M. Calligaris, G. Nardin, L. Randaccio, *Acta Crystallogr., Sect. B* **1978**, *34*, 1360–1363.
[47] V. Z. Mota, G. S. G. de Carvalho, P. P. Corbi, F. R. G. Bergamini, A. L. B. Formiga, R. Diniz, M. C. R. Freitas, A. D. da Silva, A. Cuin, *Spectrochim. Acta Part A* **2012**, *99*, 110–115.
[48] P. E. Riley, V. L. Pecoraro, C. J. Carrano, J. A. Bonadies, K. N. Raymond, *Inorg. Chem.* **1986**, *25*, 154–160.
[49] M. Gerloch, F. E. Mabbs, *J. Chem. Soc. A* **1967**, 1900–1908.
[50] S. Brückner, M. Calligaris, G. Nardin, L. Randaccio, *Acta Crystallogr., Sect. B* **1969**, *25*, 1671–1674.
[51] M. A. Siegler, M. Lutz, *Cryst. Growth Des.* **2009**, *9*, 1194–1200.
[52] N. Kumari, R. Prajapati, L. Mishra, *Polyhedron* **2008**, *27*, 241–248.
[53] W. Sawodny, U. Thewalt, E. Potthoff, *Acta Crystallogr., Sect. C* **1999**, *55*, 2060–2061.
[54] M. M. Bhadbhade, D. Srinivas, *Inorg. Chem.* **1993**, *32*, 6122–6130.
[55] M. Odoko, N. Tsuchida, N. Okabe, *Acta Crystallogr., Sect. E* **2006**, *62*, 708–709.
[56] A. F. Holleman, E. Wiberg, N. Wiberg, *Lehrbuch der Anorganischen Chemie*, 101st ed., de Gruyter, Berlin, **1995**.
[57] R. H. Thomson, *Naturally Occuring Quinones*, Academic Press, London, **1971**.
[58] P. E. Aranha, M. P. dos Santos, S. Romera, E. R. Dockal, *Polyhedron* **2007**, *26*, 1373–1382.
[59] B. Bosnich, *J. Am. Chem. Soc.* **1968**, *90*, 62.
[60] B. Ortiz, S.-M. Park, *Bull. Korean Chem. Soc.* **2000**, *21*, 405–411.
[61] O. Rotthaus, F. Thomas, O. Jarjayes, C. Philouze, E. Saint-Aman, J.-L. Pierre, *Chem. Eur. J.* **2006**, *12*, 6953–6962.
[62] P. Siega, V. Vrdoljak, C. Tavagnacco, R. Dreos, *Inorg. Chim. Acta* **2012**, *387*, 93–99.
[63] A. Kochem, H. Kanso, B. Baptiste, H. Arora, C. Philouze, O. Jarjayes, H. Vezin, D. Luneau, M. Orio, F. Thomas, *Inorg. Chem.* **2012**, *51*, 10557–10571.
[64] T. Kurahashi, H. Fujii, *Inorg. Chem.* **2013**, *52*, 3908–3919.
[65] W. L. F. Armarego, D. D. Perrin, *Purification of Laboratory Chemicals*, 4th ed., Elsevier, Burlington, **1996**.
[66] M. M. Olmstead, P. P. Power, S. C. Shoner, *Inorg. Chem.* **1991**, *30*, 2547–2551.
[67] H. Bürger, U. Wannagat, *Monatsh. Chem.* **1963**, *94*, 1007–1012.
[68] J. Chatt, M. L. Searle, *Inorg. Synth.* **1957**, *5*, 210–215.
[69] H. Bürger, W. Sawodny, U. Wannagat, *J. Organomet. Chem.* **1965**, *3*, 113–120.
[70] G. R. Fulmer, A. J. M. Miller, N. H. Sherden, H. E. Gottlieb, A. Nudelman, B. M. Stoltz, J. E. Bercaw, K. I. Goldberg, *Organometallics* **2010**, *29*, 2179–2179.
[71] *APEX2*, Bruker AXS Inc., Madison, WI, **2007**; *SAINT*, Bruker AXS Inc., Madison, WI, **2007**.
[72] *X-AREA*, Stoe & Cie, Darmstadt, Germany, **2002**; *X-RED*, Stoe & Cie, Darmstadt, Germany, **2002**.
[73] L. J. Farrugia, *J. Appl. Crystallogr.* **2012**, *45*, 849–854.

[74] A. Altomare, M. C. Burla, M. Camalli, G. L. Cascarano, C. Giacovazzo, A. Guagliardi, A. G. G. Moliterni, G. Polidori, R. Spagna, *J. Appl. Crystallogr.* **1999**, *32*, 115–119.
[75] G. M. Sheldrick, *Acta Crystallogr., Sect. A* **2008**, *64*, 112–122.
[76] A. L. Spek, *Acta Crystallogr., Sect. D* **2009**, *65*, 148–155.
[77] R. H. Blessing, *Acta Crystallogr., Sect. A* **1995**, *51*, 33–38.
[78] *SADABS*, v. 2012/1, Bruker AXS Inc., Madison, WI, **2012**.
[79] K. Brandenburg, *DIAMOND*, Crystal Impact GbR, Bonn, Germany, **1999**.

Received: November 20, 2015
Published Online: January 5, 2016